Comparison of inclusive charged-pion production in $\pi^{\pm}p$ interactions at 100 GeV/c

J. Whitmore, B. Y. Oh, M. Pratap, G. Sionakides, and G. A. Smith
*Department of Physics, Michigan State University, East Lansing, Michigan 48824**

V. E. Barnes, D. D. Carmony, R. S. Christian, A. F. Garfinkel, W. M. Morse,† and L. K. Rangan
Department of Physics, Purdue University, West Lafayette, Indiana 47907‡

L. Voyvodic and R. Walker
Fermi National Accelerator Laboratory, Batavia, Illinois 60510‡

E. W. Anderson, H. B. Crawley, A. Firestone, W. J. Kernan, and D. L. Parker
Ames Laboratory—ERDA and Department of Physics, Iowa State University, Ames, Iowa 50010‡

R. G. Glasser, D. G. Hill,§ M. Kazuno, G. McClellan, H. L. Price, B. Sechi-Zorn, G. A. Snow, and F. Svreck
Department of Physics, University of Maryland, College Park, Maryland 20742‡

A. R. Erwin, E. H. Harvey, R. J. Loveless, and M. A. Thompson
Department of Physics, University of Wisconsin, Madison, Wisconsin 53706‡

(Received 6 June 1977)

Inclusive single-particle spectra for $\pi^{\pm}$ production are presented for data from $\pi^{\pm}p$ interactions at 100 GeV/c. The spectra for the four reactions $\pi^{\pm}p \to \pi^{\pm}$ + anything are compared as a function of laboratory longitudinal momentum, Feynman x, center-of-mass (c.m.) rapidity, and transverse momentum squared. Comparisons are also made between these data and analogous data from 16 and 18.5 GeV/c $\pi^{\pm}p$ interactions and the energy dependence is discussed. Average values of the transverse momentum are given as a function of the longitudinal momentum and charged-particle multiplicity. A comparison of the charge distributions is presented as a function of rapidity and c.m. energy.

I. INTRODUCTION AND DEFINITIONS

Inclusive charged-pion production in $\pi^{\pm}p$ interactions has been studied extensively at incident-beam momenta below ~25 GeV/c (Ref. 1–3) and a preliminary analysis of the leading particle effect in $\pi^{-}p$ interactions at 100 GeV/c has recently been published.[4] In this paper we present a comprehensive study of $\pi^{\pm}$ production in 100 GeV/c $\pi^{\pm}p$ interactions as observed in the Fermi National Accelerator Laboratory (Fermilab) 30-inch hydrogen bubble chamber. In order to obtain increased accuracy on the momentum determination for fast forward-going charged particles we have made use of the wide-gap optical spark-chamber hybrid system. This system provides unbiased detection of charged secondaries in all regions of phase space.

The data are presented in terms of four common variables: (a) The longitudinal component of the laboratory momentum, p_L; (b) the Feynman reduced center-of-mass (c.m.) longitudinal momentum, $x = P_L^*/P_{\max}^* \approx 2P_L^*/\sqrt{s}$; (c) the c.m. longitudinal rapidity, $y^* = \frac{1}{2}\ln[(E^* + P_L^*)/(E^* - P_L^*)]$ (where the superscript asterisk refers to c.m. quantities); and (d) the square of the transverse momentum, p_T^2. In terms of these variables the invariant distribution function, or structure function, has the forms:

$$f(\vec{p}, s) = E\frac{d^3\sigma}{dp^3} = \frac{E}{\pi}\frac{d^2\sigma}{dp_L dp_T^2}\,, \tag{1a}$$

$$= \frac{1}{\pi p_{\max}^*} E^* \frac{d^2\sigma}{dx dp_T^2}\,, \tag{1b}$$

$$= \frac{1}{\pi}\frac{d^2\sigma}{dy^* dp_T^2} \tag{1c}$$

For convenience in discussing the reactions,

$$\pi^- p \to \pi^- + \text{anything}\,, \tag{2}$$

$$\pi^- p \to \pi^+ + \text{anything}\,, \tag{3}$$

$$\pi^+ p \to \pi^- + \text{anything}\,, \tag{4}$$

and

$$\pi^+ p \to \pi^+ + \text{anything}\,, \tag{5}$$

we follow the notation of Bosetti *et al.*[1] and let f_{ac} denote the structure function for the process $\pi^a p \to \pi^c$ + anything, where the first subscript refers to the charge of the beam particle and the second subscript refers to the charge of the produced pion.

In Sec. II we discuss the experimental details and data sample used for analysis. In Sec. III the longitudinal distributions are presented, and from a comparison with other published data the energy

TABLE I. Number of events and cross sections used.

n_c	100 GeV/c π^-p Events	100 GeV/c π^-p σ_n (mb) (Ref. 5)	100 GeV/c π^+p Events	100 GeV/c π^+p σ_n (mb) (Ref. 8)
inel 2	382	1.95	272	2.38
4	794	4.79	619	4.65
6	972	5.17	662	4.82
8	790	4.30	489	3.63
10	450	2.50	362	2.64
12	228	1.41	176	1.25
14	76	0.60	66	0.49
16	30	0.133	21	0.13
18	7	0.045	6	0.04
20	...	0.014	2	0.02
22	1	0.008	...	...
Totals	3730	20.92	2675	20.05

dependence of $\pi^\pm$ production in $\pi^\pm p$ interactions is studied. The properties of the transverse-momentum distributions and the correlation between $\langle p_T \rangle$ and x (or y) are discussed in Sec. IV. In Sec. V, we study the charge distributions in these data. Section VI presents a summary of the main conclusions.

II. EXPERIMENTAL DETAILS AND DATA SAMPLE

The data presented in this paper come from four separate exposures of the Fermilab 30-inch hydrogen bubble chamber to 100 GeV/c pion beams. The first π^- and π^+ exposures of 53 000 and 104 000 pictures, respectively, were taken by the CERN[5] and Davis-LBL[6] groups, and, following agreements with Fermilab, the bubble-chamber photographs were later given[7] to the present groups in order to combine the bubble-chamber data with the information from the downstream spark chambers. The second exposures of 56 000 π^-p and 83 000 π^+p pictures were taken by the present groups. All of the π^+p data in this paper have been measured and analyzed by the Purdue-Wisconsin group,[8] and the π^-p data have been obtained by the Michigan State–Fermilab–Iowa State–Maryland Collaboration. The numbers of $\pi^\pm p$ events used in this analysis are shown in Table I along with the cross sections that have been used for normalization. For both experiments, the elastic events have been removed after determination by kinematic fitting. All negative particles are assumed to be π^-, protons with laboratory momenta less than 1.4 GeV/c have been identified by ionization in the bubble chamber, and all remaining positive particles are assumed to be π^+. We estimate that about 70% of all protons have been identified by ionization. The remainder comprise about 5% of all unidentified positive tracks and have a negligible effect on our conclusions unless explicitly noted.

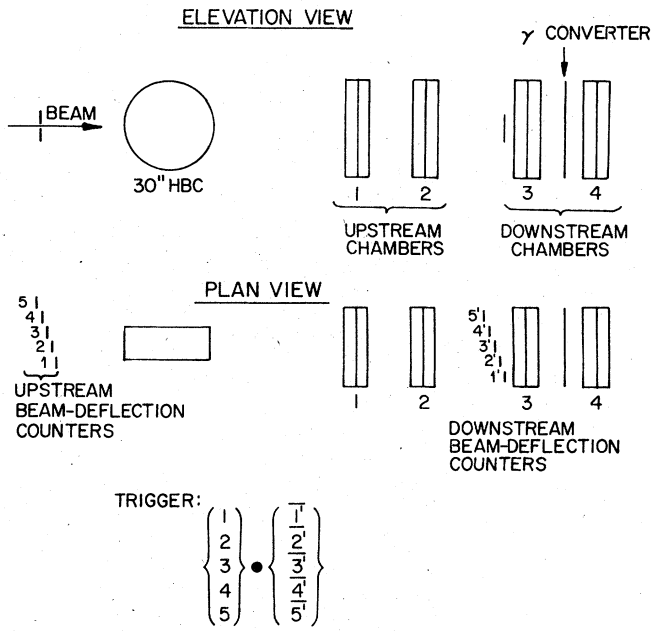

FIG. 1. Schematic view of the 30-inch bubble-chamber and wide-gap spark-chamber hybrid system.

The particle identification in the positive beam was determined by a 34-m-long differential Čerenkov counter located 400 m upstream from the 30-inch bubble chamber. The ratios found were 46% π^+, 1.5% K^+, 50% p, and 2.7% μ^+.[9] Each π^+p event used in this analysis has been uniquely identified as a π^+ interaction using the Čerenkov counter in conjunction with the upstream proportional-wire-counter beam-tagging system. For the π^-p experiment, the contamination due to nonpion interactions is less than a few percent and has been ignored.

The downstream wide-gap optical spark-chamber system[10] is shown schematically in Fig. 1. The four dual-gap spark chambers were triggered, as shown in Fig. 1, either by a deflected (interacting) beam track or by a secondary multiplicity trigger corresponding to two or more particles in a scintillator measuring the energy loss. On typical secondary tracks this system yields a $\Delta p/p \sim \pm(4\times10^{-4})p$ (where p is in GeV/c). Since some of the forward-going tracks interact in the downstream hydrogen or the bubble-chamber windows and since there is an inefficiency due to the spark-chamber dead time, not all events with fast forward-going particles have spark-chamber information. In order to obtain the best resolution possible in the beam-fragmentation region, we use only those tracks which have complete bubble-chamber and spark-chamber information merged together (hooked up).

For the π^-p data we have used only those tracks which have both bubble-chamber and spark-cham-

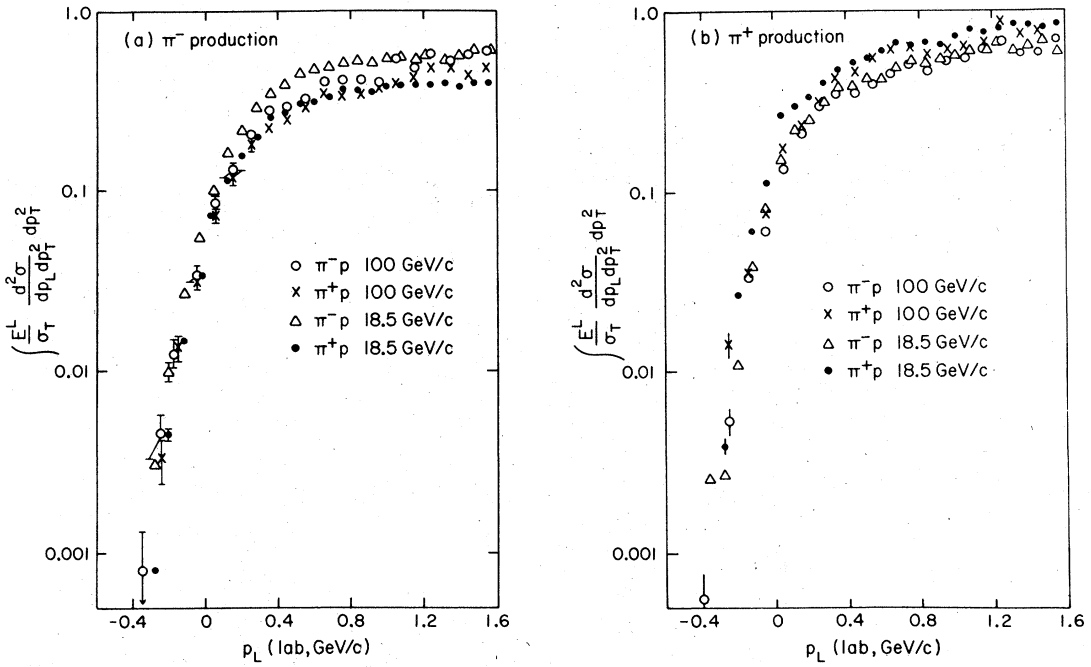

FIG. 2. Invariant cross section as a function of the longitudinal laboratory momentum for (a) π^- and (b) π^+ production in 18.5 and 100 GeV/c $\pi^{\pm}p$ interactions.

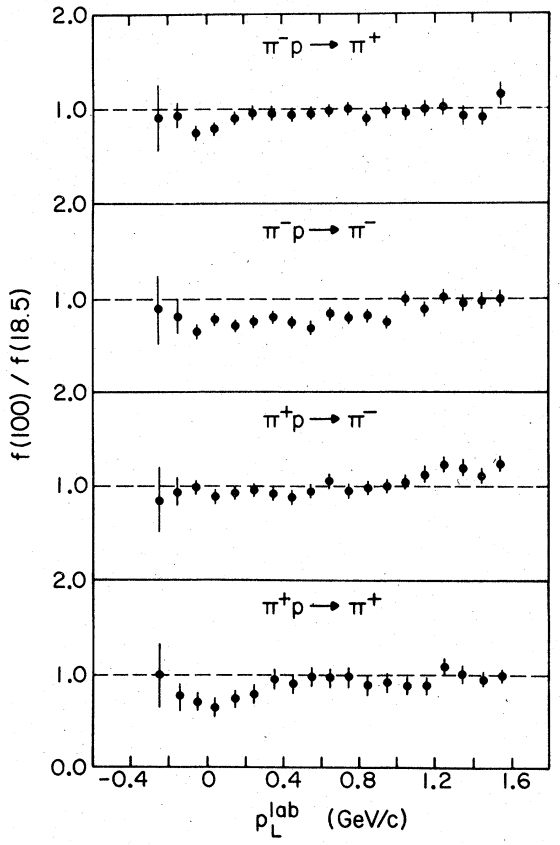

FIG. 3. Ratios of the invariant cross sections at 100 and 18.5 GeV/c as a function of the longitudinal laboratory momentum.

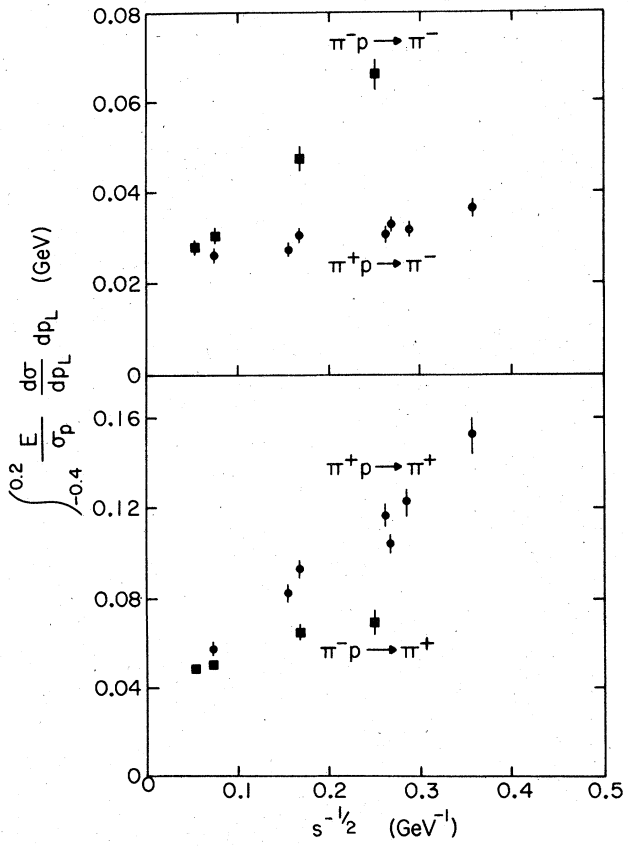

FIG. 4. The invariant cross section integrated over the range $-0.4 < p_L < 0.2$ GeV/c as a function of $s^{-1/2}$.

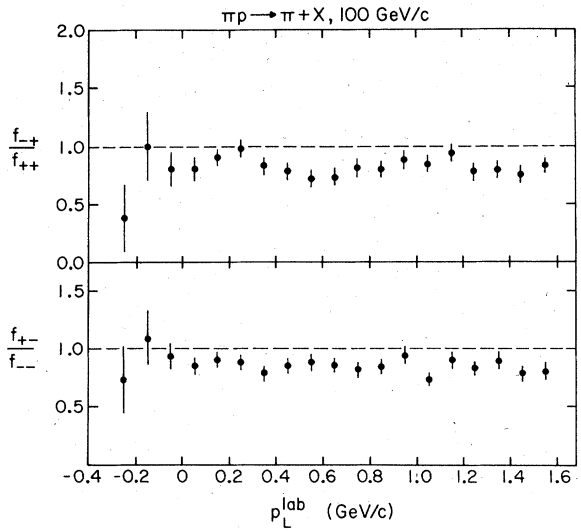

FIG. 5. Ratio of the invariant cross sections for $\pi^- p$ and $\pi^+ p$ interactions at 100 GeV/c as a function of the longitudinal laboratory momentum.

ber data for values of $x \geq 0.55$. The normalization in this region is obtained by assuming that the integrated inclusive cross section for $x \geq 0.55$ is given by the bare chamber data for $x \geq 0.55$. Owing to the limited statistics in this region (≈150 hooked-up tracks), this procedure is quite adequate. For the $\pi^+ p$ events, we have only used hooked-up tracks for $x \geq 0.2$ and each track is weighted[8] according to the overall hookup acceptance as obtained from a study of 100 GeV/c pp events from the same exposure and by invoking the symmetry of the pp interaction in the center-of-mass system.

III. LONGITUDINAL DISTRIBUTIONS

In this section we integrate over all transverse momenta and discuss the data in terms of the dependence on longitudinal variables.

A. Target-fragmentation region

We first consider pion production in the target-fragmentation region. It has been suggested by Benecke *et al.*[11] that the spectra of produced particles in the kinematic region where the produced

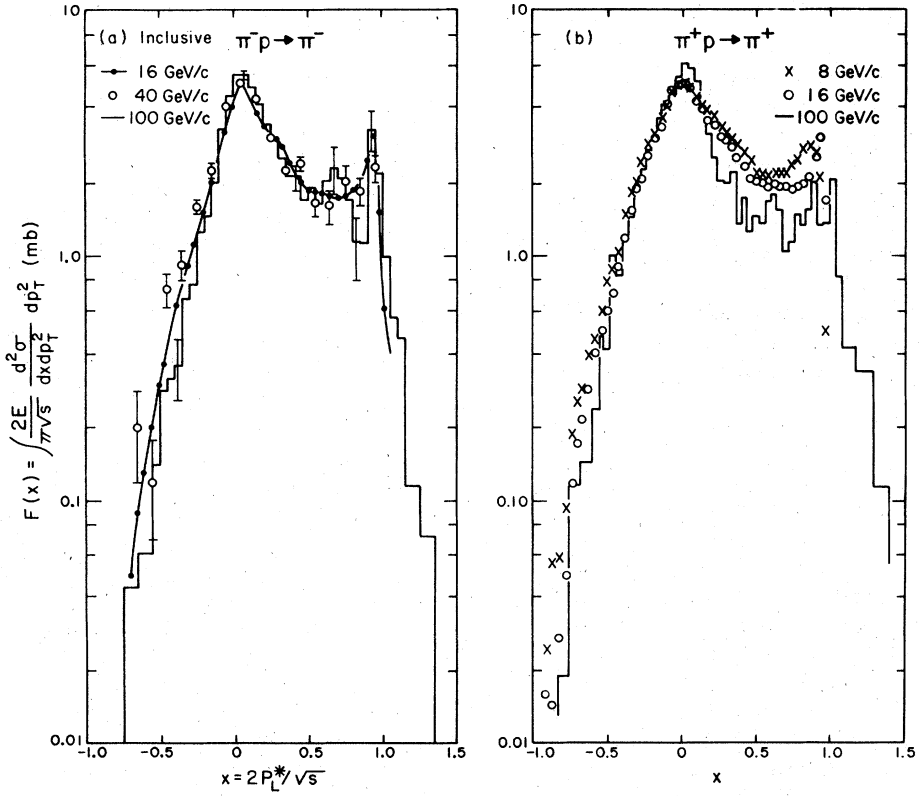

FIG. 6. Invariant cross section as a function of the Feynman x variable for (a) $\pi^- p \to \pi^-$ and (b) $\pi^+ p \to \pi^+$. Elastic events have been removed.

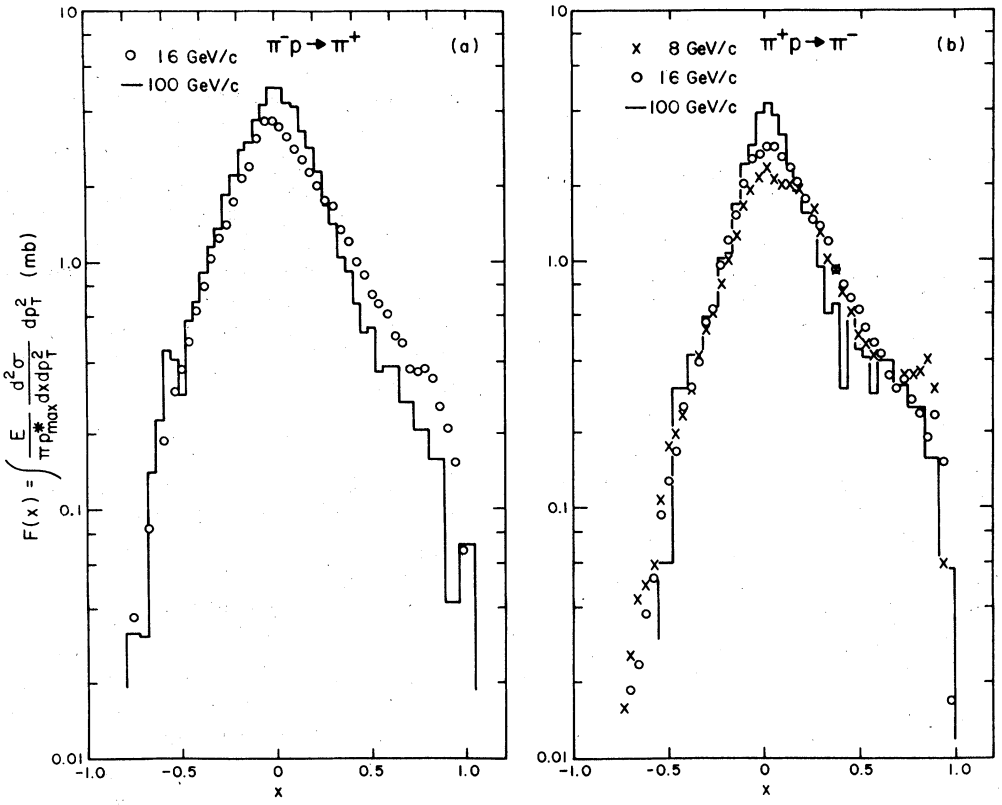

FIG. 7. Invariant cross section as a function of the Feynman x variable for (a) $\pi^- p \to \pi^+$ and (b) $\pi^+ p \to \pi^-$.

particle has a small momentum in the rest frame of the target should become independent of the total c.m. energy, $\sqrt{s}$, as $\sqrt{s}$ becomes very large. This is the hypothesis of limiting fragmentation. A recent study[12] of $\pi^\pm$ production in pp interactions has shown that if such an energy independence does occur it must happen at energies above those currently attainable at Fermilab. In order to test this hypothesis in $\pi^\pm p$ interactions, we show in Figs. 2(a) and 2(b) the π^- and π^+ structure functions, integrated over all $p_T{}^2$ and normalized to the total cross sections:

$$\int \frac{E}{\sigma_T} \frac{d^2\sigma}{dp_L dp_T{}^2} dp_T{}^2 , \tag{6}$$

as a function of p_L for $\pi^\pm p$ data at both 100 and 18.5 GeV/c.[2] These plots show that for the beamlike pion-production reactions, (2) and (5), there is a strong energy dependence with the low-energy data showing larger cross sections. For the nonbeamlike pion production the energy dependence is much weaker although the cross sections still show a slight decrease with increasing beam momentum. This energy dependence is shown explicitly in Fig. 3, where the ratio of the cross section at 100 GeV/c to that at 18.5 GeV/c is plotted as a function of p_L for the four processes (2–5). The two reactions in which the produced particle and the beam particle are identical show a stronger dependence on $\sqrt{s}$ than reactions (3) and (4).

To investigate the functional form of the $\sqrt{s}$ dependence in more detail, we integrate over the region $-0.4 \leq p_L \leq 0.2$ GeV/c and plot the integrated cross section versus $s^{-1/2}$. The results are shown in Fig. 4, where they are compared with all available data.[13] Note that the cross sections in Fig. 4 have been normalized by σ_p, the Pomeron contribution to the total cross section at each beam momentum as parametrized by Quigg[14]:

$$\sigma_p(p_{\rm lab}) = (15.18 \text{ mb}) p_{\rm lab}{}^{0.0755} . \tag{7}$$

Figure 4 shows clearly the effects seen in Figs. 2 and 3, namely that all cross sections decrease with $\sqrt{s}$ and that reactions (2) and (5) have the strongest energy dependence. The data on the four processes shown in Fig. 4 appear to be compatible with a linear dependence on $s^{-1/2}$ as predicted by Chan *et al.*[15] and by Miettinen.[16] In fact, a recent study[17] of all the available data on $\pi^\pm$ production in NN, KN, and πN interactions has shown that these data are in good agreement with the predictions of Chan *et al.* The data shown in Fig. 4 clearly demonstrate that if the hypothesis of limiting fragmentation is valid it must be true only

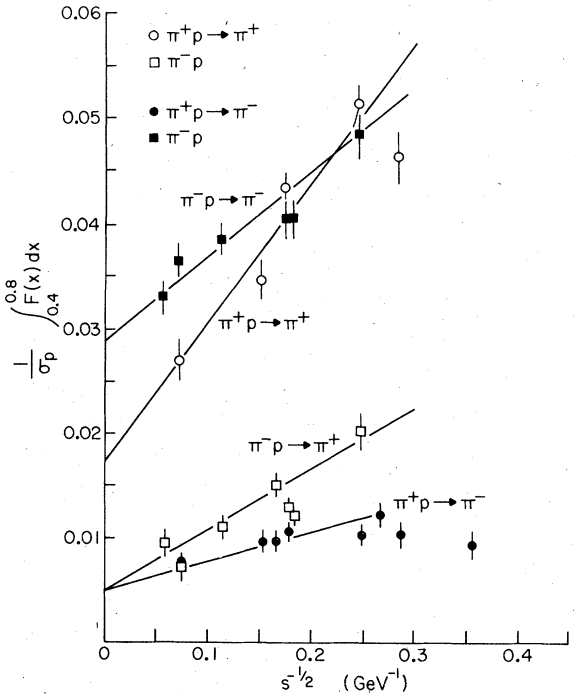

FIG. 8. The invariant cross section integrated over the range $0.4 < x < 0.8$ as a function of $s^{-1/2}$.

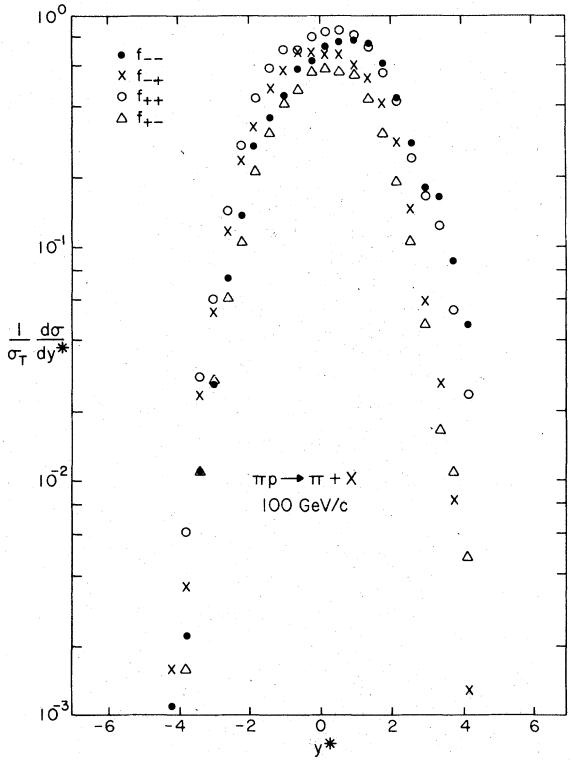

FIG. 9. Rapidity spectrum, normalized to the total πp cross section, for the reactions $\pi^\pm p \to \pi^\pm$ + anything at 100 GeV/c.

for energies exceeding those for which data are currently available.

Figure 5 shows the ratios of the structure functions, f_{-+}/f_{++} and f_{+-}/f_{--}, at 100 GeV/c as a function of p_L. It is clear that the rates for π production at 100 GeV/c are sensitive to the nature of the beam even for produced pions that are very slow in the laboratory and that the ratios appear constant over the range $-0.2 \leq p_L \leq 1.6$ GeV/c.

B. Beam-fragmentation region

Figures 6 and 7 show the π^+ and π^- inclusive Feynman x distributions for our 100 GeV/c data compared to data at 8 and 16 GeV/c (Ref. 1) and at 40 GeV/c.[18] Figure 6 shows that the spectra for beamlike pions are similar in both shape and magnitude. The dominant feature is the peaking near $x = +1$. This peak arises from the diffractive excitation of the target proton. We have shown elsewhere[4] that the inelastic two-prong events are the dominant contributions to this peak. It should be noted, however, that the elastic events which would also populate this region have been removed. Figure 7 shows that for the nonbeam-like pion spectra there is no peak for p_{lab} greater than 16 GeV/c but that the asymmetry about $x = 0$ is still a dominant feature of the distribution. The larger forward-c.m.-hemisphere cross sections are due to diffractive excitation of the beam pion.[19]

Other features apparent in Figs. 6 and 7 are the decreasing cross sections in the target-fragmentation region (as discussed in detail above) and in the beam-fragmentation region ($x \gtrsim 0.4$) as the incident momentum increases. The latter feature is shown more clearly in Fig. 8. In order to make a comparison with previously published data at lower energies[13] the inclusive single-particle spectra have been integrated over the region $0.4 \leq x \leq 0.8$ and again normalized to σ_p as in Eq. (7). In this region, processes (2) and (5) are dominated by diffractive excitation of either target or beam (mostly the latter) and show a strong energy dependence. The reactions (3) and (4) behave in a manner similar to the target fragmentation data, i.e., they fall slowly with increasing energy and are consistent with a common cross section at infinite energy.

C. Central-region production

For the study of central-region pion production, the most suitable variable is the c.m. rapidity y^*. A well-known feature of $\pi^\pm$ production in pp interactions is the rise of the cross section at $y^* = 0$.[20] Central-region pion production may now be studied in high-energy $\pi^\pm p$ interactions.

A comparison of the rapidity spectra for reactions (2)–(5) is shown in Fig. 9. In the central region, the values of the cross section are strongly dependent on the charge of the incident and pro-

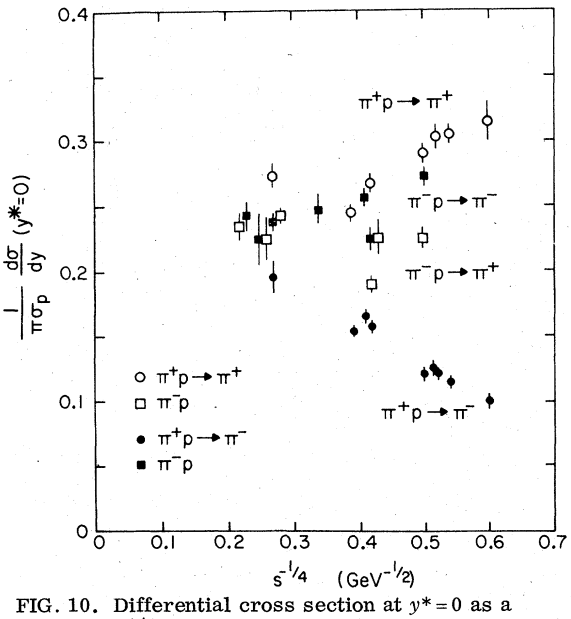

FIG. 10. Differential cross section at $y^*=0$ as a function of $s^{-1/4}$.

duced pions. The cross sections for producing pions with the same charge as the beam ("favored") are significantly larger than those for pions produced with the opposite charge to that of the beam particle ("unfavored").

Figures 6 and 7 also show that the $\pi^\pm$ cross sections near $x=0$ are rising with energy and that the effect is larger for the nonbeamlike reactions (3)

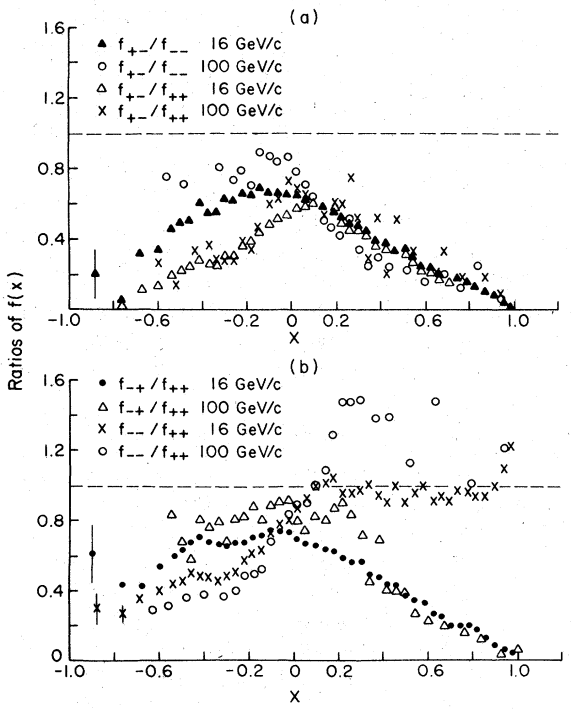

FIG. 11. Ratios of $\pi^\pm$ production cross sections as a function of x at 16 and 100 GeV/c.

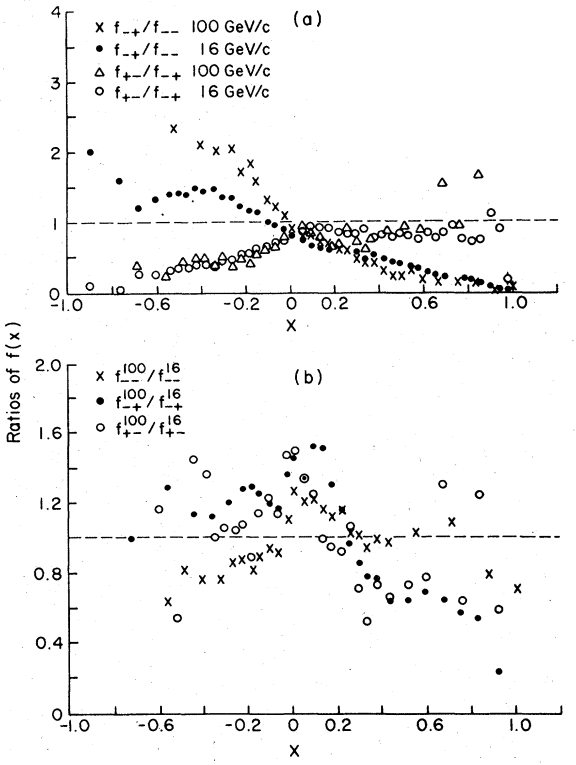

FIG. 12. Ratios of $\pi^\pm$ production cross sections as a function of x at 16 and 100 GeV/c.

and (4) than for processes (2) and (5) where a strong leading-particle effect can exist. The energy dependences of these cross sections[13] are shown in Fig. 10 (Ref. 20) where the cross-section $d\sigma/dy$, evaluated at $y^*=0$, is plotted as a function of $s^{-1/4}$ which is the energy dependence expected from the Mueller-Regge phenomenology.[21] Note that the cross sections have again been normalized by σ_p, Eq. (7). The dominant features of Fig. 10 are the following:

(a) The cross section for $\pi^+p\to\pi^-$ rises almost linearly with decreasing $s^{-1/4}$ in much the same

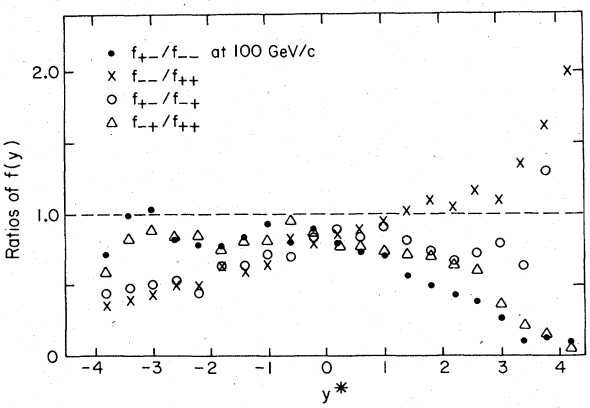

FIG. 13. Ratios of $\pi^\pm$ production cross sections as a function of the c.m. rapidity at 100 GeV/c.

way as $pp \to \pi^{\pm}$.[20]

(b) The cross sections for $\pi^+p \to \pi^+$ and $\pi^-p \to \pi^-$ appear to fall with increasing beam momentum from the lowest energy studied (at $P_{\text{lab}} = 3.7$ GeV/c) to about $s^{-1/4} \approx 0.27$ ($P_{\text{lab}} = 100$ GeV/c). The highest-energy data (for $P_{\text{lab}} \gtrsim 100$ GeV/c) appear to be approximately independent of $s^{-1/4}$ and have about the same magnitude as the $\pi^+p \to \pi^-$ data.

(c) The trend of the $\pi^-p \to \pi^+$ data is somewhat unclear at the lower energies but this process has approximately the same magnitude for $P_{\text{lab}} \geq 100$ GeV/c as the other three processes.

The decrease at $y^* = 0$ for reactions (2) and (5) may be understood in terms of the decreasing contribution of the diffractive-excitation process to the central-region cross section. As seen in Fig. 6 the diffractive peak near $x = +1$ appears to be moving towards the kinematic limit ($x = +1$).[4] Presumably, at higher energies the $y^* = 0$ cross section for these two reactions will begin to increase in much the same way as observed for $pp \to \pi^{\pm}$ and $\pi^+p \to \pi^-$.

D. Comparison of $\pi^{\pm}p$ interactions

In Figs. 11 and 12 various ratios are plotted as a function of the Feynman x variable for reactions (2)–(5) at 16 (Ref. 1) and 100 GeV/c. Figure 13 shows the ratios at 100 GeV/c as a function of rapidity. The dominant features of these plots are the following:

(i) *For beamlike (favored) pion production:*

(a) At 16 GeV/c (Ref. 1) it was found that the leading-particle cross sections in $\pi^{\pm}p \to \pi^{\pm}$ are quite similar in the forward hemisphere where f_{--}/f_{++} ranges from 0.9 to 1.0 for $0.1 \lesssim x \lesssim 0.9$ [see Fig. 11(b)]. At 100 GeV/c, f_{--}/f_{++} is consistently above 1.0 for $x > 0.1$ ($y^* > 1.5$).

(b) For $x \gtrsim 0.9$, it appears that f_{--}/f_{++} rises rapidly at both 16 and 100 GeV/c [Figs. 11(b) and 13].

(c) In the backward hemisphere, the f_{++} cross sections are larger than f_{--} at both 16 and 100 GeV/c. This is presumably due to the equal charges of the π^+ and target proton. The ratio of f_{--}/f_{++} is falling with increasing c.m. energy [Fig. 11(b)].

(d) The ratio of f_{--} at 100 GeV/c to that at 16 GeV/c shows [Fig. 12(b)] that the cross section is falling for $x \lesssim -0.1$ and $x \gtrsim 0.7$ (as was discussed above) and is rising near $x = 0$.

(ii) *For nonbeamlike (unfavored) pion production:*

(a) The ratio of f_{-+}/f_{++} is almost independent of c.m. energy for $x \gtrsim 0.4$ but rises with increasing energy for $x \lesssim 0.4$ [Fig. 11(b)].

(b) As a function of energy, f_{+-}/f_{--} rises for $x \lesssim 0.1$, falls slightly for $0.1 \lesssim x \lesssim 0.6$, and is approximately constant for $x \gtrsim 0.6$ [Fig. 11(a)].

(c) In the backward hemisphere, f_{-+}/f_{++} and f_{+-}/f_{--} are both smaller than unity at both energies [Figs. 11(a) and 11(b), Fig. 13] suggesting that the charge of the beam still affects the $\pi^{\pm}$ production cross sections in the target-proton–fragmentation region at 100 GeV/c. Both ratios are increasing towards unity as the beam momentum is increased from 16 to 100 GeV/c.

(d) The ratio of f_{+-}/f_{++} shows no energy dependence for $|x| \gtrsim 0.2$, but is increasing for $|x| \lesssim 0.2$ as the incident-beam momentum increases from 16 to 100 GeV/c [Fig. 11(a)].

(e) The ratio f_{+-}/f_{-+} shows no energy dependence throughout the entire x range [Fig. 12(a)].

(f) For $x \lesssim 0.2$, the ratio f_{-+}/f_{--} rises steadily as x becomes smaller and as the energy increases. For $x \gtrsim 0.2$, the opposite is true, although the energy dependence is not as strong. The forward hemisphere data reflect the fact that f_{-+} falls more rapidly with increasing energy than f_{--} which is dominated by diffractive excitation. The conclusion to be drawn from Figs. (11)–(13) for the 100-GeV/c data is similar to that found at 16 GeV/c (Ref. 1), i.e., that the charge of the incident pion appears to have a longer-range effect than the charge of the proton.

IV. TRANSVERSE-MOMENTUM DISTRIBUTIONS

Figure 14 shows the transverse-momentum distributions for the four processes at 100 GeV/c. All four reactions have a similar shape although there is some evidence that f_{++} is increasing with respect to f_{+-} at the higher p_T^2 values. This is shown in more detail in Fig. 15 where various ra-

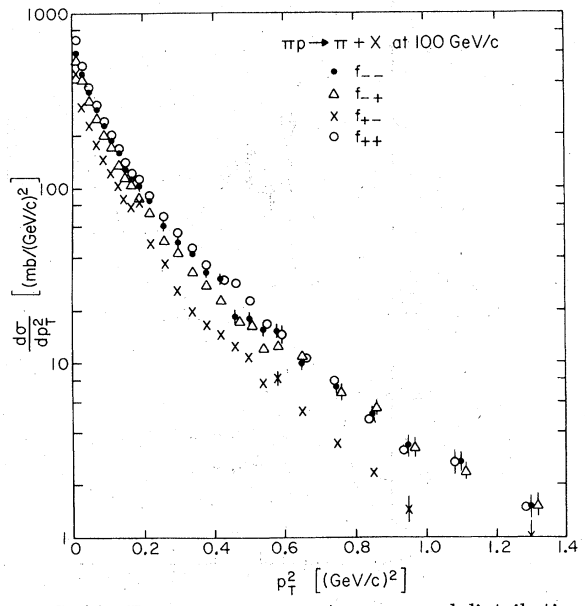

FIG. 14. Transverse-momentum-squared distributions for $\pi^{\pm}$ production at 100 GeV/c.

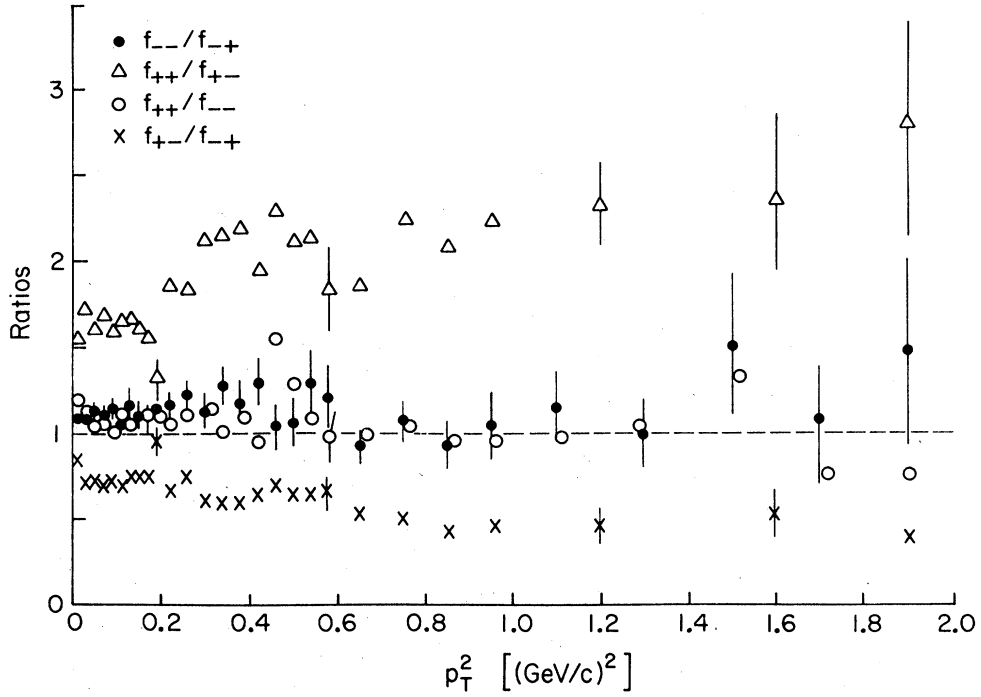

FIG. 15. Ratios of $\pi^{\pm}$ production cross sections as a function of p_T^2 at 100 GeV/c.

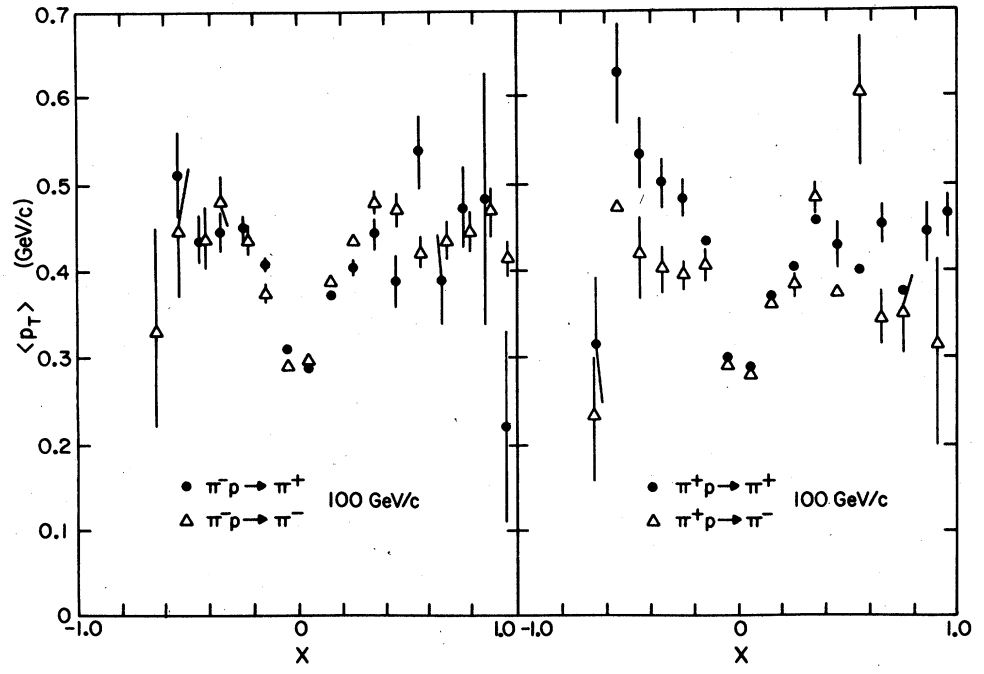

FIG. 16. Average values of the transverse momentum as a function of x for $\pi^- p$ interactions at 100 GeV/c.

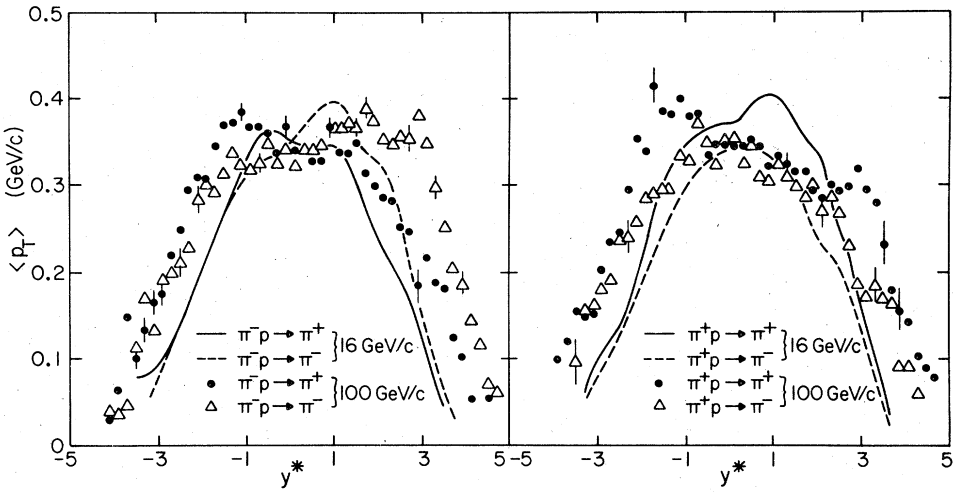

FIG. 17. Average values of the transverse momentum as a function of the c.m. rapidity for $\pi^{\pm}p$ interactions at 16 and 100 GeV/c.

tios are given as a function of p_T^2. In addition to the increase of f_{++}/f_{+-}, f_{+-}/f_{-+} shows a slight decrease while f_{--}/f_{-+} and f_{++}/f_{--} appear to be equal and independent of p_T^2. It is clear from Fig. 14 that a simple exponential function in p_T^2 cannot describe these data.

A. Longitudinal- and transverse-momentum correlations

In Figs. 16 and 17 we show the average values of p_T for the four reactions (2)–(5) at 100 GeV/c. The well-known "seagull" effect is strong in our data with the decrease in $\langle p_T \rangle$ near $x=0$ occurring in all four processes when $\langle p_T \rangle$ is plotted versus x. When $\langle p_T \rangle$ is plotted versus y^*, Fig. 17, no such effect is observed. The other main features of these figures are as follows:

(a) For $\pi^- p$ interactions at 100 GeV/c, the values of $\langle p_T \rangle$ for π^+ are larger than for π^- in most of the backward c.m. hemisphere, and vice versa in the forward hemisphere.

(b) As a function of the incident-beam momentum, the maximum value for $\langle p_T \rangle$ does not appear to increase. However, Fig. 17 shows that from 16 to 100 GeV/c, the distribution broadens as a function of y^* but otherwise keeps a similar shape.

(c) The value for $\langle p_T \rangle$ for f_{-+} peaks near $y=-1.2$ while $\langle p_T \rangle$ for f_{--} peaks near $y=+2$. A similar effect is observed in the 16 GeV/c $\pi^- p$ data (Fig. 17). The f_{++} data show a definite energy dependence with the peak in $\langle p_T \rangle$ moving from $y \simeq +1$ to $y \simeq -1$ as the beam momentum increases from 16 to 100 GeV/c.

B. Charge-multiplicity dependence of $\langle p_T \rangle$

The dependence of $\langle p_T \rangle$ on the charge multiplicity is shown in Fig. 18 where a comparison is made with data at 8.05 and 18.5 GeV/c (Ref. 2). There is a clear dependence on the incident-beam momentum with $\langle p_T \rangle_n$ increasing with higher beam energy for fixed n, and the decrease in $\langle p_T \rangle$ with n becoming less strong as the beam energy rises.

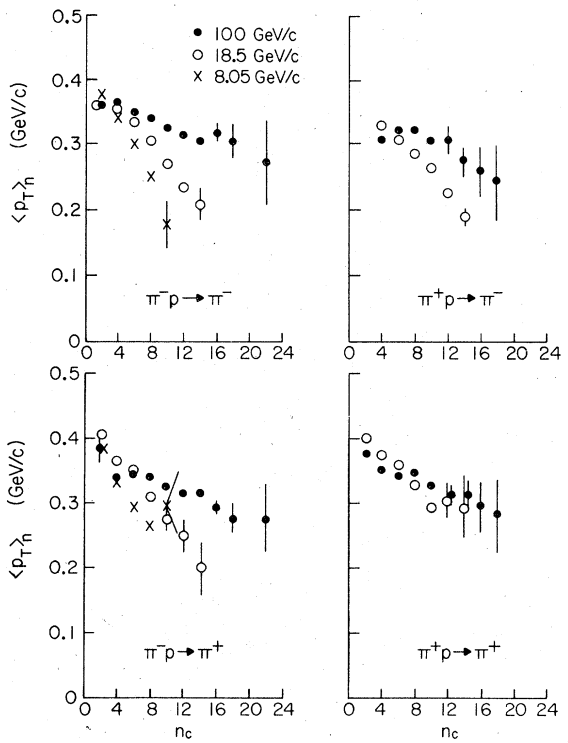

FIG. 18. Average values of the transverse momentum as a function of the associated-charged-particle multiplicity at 8, 18.5, and 100 GeV/c.

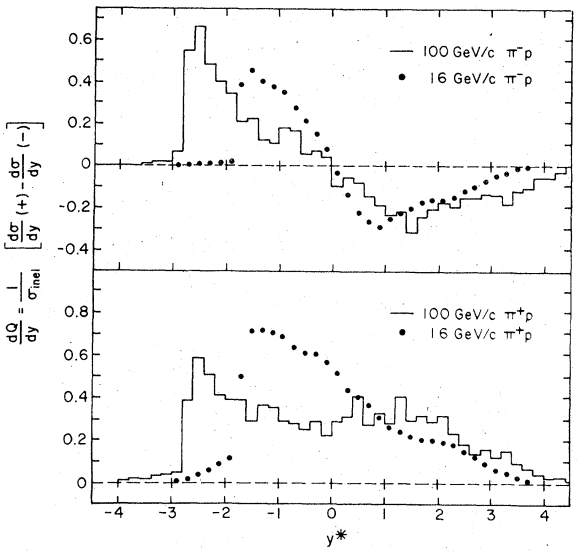

FIG. 19 Charge distributions in 16- and 100-GeV/c $\pi^{\pm}p$ interactions as a function of the c.m. rapidity.

V. CHARGE DISTRIBUTIONS

In this section we investigate the distributions of charge as a function of y^* for $\pi^{\pm}p$ interactions at 100 GeV/c. By studying such distributions one may hope to study the processes of target-proton and beam-pion fragmentation in a model-independent way. At infinite energies one might expect the charges carried by the incident projectile and target to remain in their fragmentation regions and not to extend into the central region. Furthermore, one can study the extent to which these charged fragments behave in an energy-independent way. Figure 19 shows the average charge deposited in a given rapidity interval, dQ/dy, as a function of y^* for $\pi^{\pm}p$ interactions at 16 (Ref. 22) and 100 GeV/c. To compute dQ/dy, we have included all charged particles, including identified protons, and then subtracted the rapidity spectra for negatively charged secondaries from that for positive secondaries and normalized by the inelastic cross section (Table I):

$$\frac{dQ}{dy}=\frac{1}{\sigma_{\text{inel}}}\left[\frac{d\sigma}{dy}(+)-\frac{d\sigma}{dy}(-)\right]. \tag{9}$$

With such a normalization we obtain $\int(dQ/dy)dy = 0$ (+2) for π^-p (π^+p) interactions at any energy. Figure 19 shows that target and beam fragmentation are tending to be concentrated at larger $|y^*|$ values as the incident-beam momentum increases. It also appears that the maximum value of dQ/dy in the target-fragmentation region is increasing (decreasing) with increasing beam momentum for π^-p (π^+p) interactions.

To investigate the separate effects of target and projectile fragmentation, we next form linear combinations of the charge distributions for $\pi^{\pm}p$ interactions:

$$\sum{}^{\pm}=\frac{1}{2}\left[\frac{dQ}{dy}(\pi^+p)\pm\frac{dQ}{dy}(\pi^-p)\right]. \tag{10}$$

The distributions for $\sum^{\pm}$ as a function of y^* are shown in Fig. 20, again for both 16 and 100 GeV/c. Once more, we note the tendency for the target and projectile charge fragments to be concentrated at larger values of $|y^*|$. The shape of the π fragmentation [Fig. 20(a)] appears to be energy independent, while the target-proton fragmentation does show a change from 16 to 100 GeV/c; although it is possible that this is a result of differences in the kinematic regions for (slow) proton identification at the two energies.

Also clearly apparent in Fig. 20 is the fact that the proton charge fragmentation distribution, Fig. 20(b), is narrower than the π charge fragmentation spectrum. A similar effect has been observed in 10 and 16 GeV/c K^-p interactions.[23] Finally, we note that the extent of the two charge distributions, with both fragments extending about 2 units past $y^*=0$, is such that even at 100 GeV/c there is no neutral central region observed.

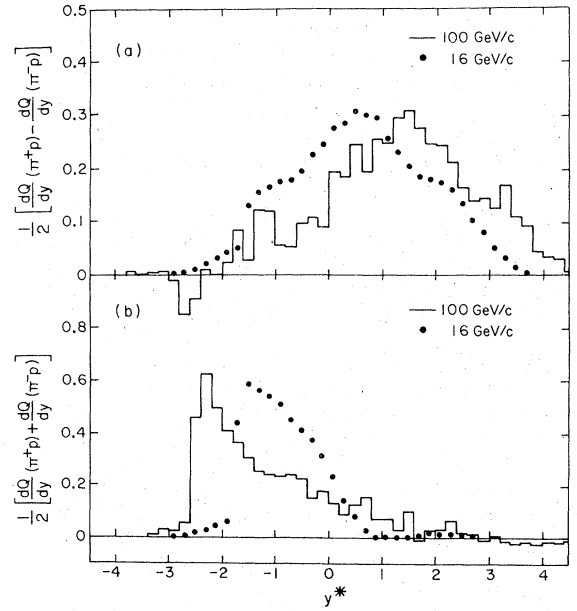

FIG. 20 (a) The difference and (b) the sum of the charge distributions in π^+p and π^-p interactions at 16 and 100 GeV/c as a function of the c.m. rapidity.

VI. SUMMARY OF RESULTS

From the distributions presented here for inclusive $\pi^{\pm}$ production in π^-p and π^+p interactions at 100 GeV/c, and from comparisons with data at other energies, we find the following:

(a) Unfavored fragmentation in both the target- and projectile-fragmentation regions displays a weaker energy dependence than favored fragmentation, although both reactions exhibit an $s^{-1/2}$ behavior. We note that in the projectile-fragmentation region the asymptotic cross sections for f_{--} and f_{++} are not the same, and both are different from the $s=\infty$ cross sections for f_{+-} and f_{-+}.

(b) Central-region production for f_{+-} rises linearly with $s^{-1/4}$ while f_{--} and f_{++} decrease and then approach the values for f_{+-} and f_{-+}.

(c) The ratio f_{+-}/f_{++} is energy independent in the backward c.m. hemisphere, others (e.g., f_{-+}/f_{++}, f_{-+}/f_{--}) are energy independent in the forward hemisphere, while f_{+-}/f_{-+} shows no energy dependence anywhere.

(d) The $p_T{}^2$ distributions are relatively insensitive to the charges of incident and produced pions; although some increase in the ratio f_{++}/f_{+-} is observed as $p_T{}^2$ increases.

(e) The correlation between p_T and the longitudinal variables shows the seagull effect when $\langle p_T \rangle$ is plotted as a function of x but not when plotted versus y^*.

(f) $\langle p_T \rangle$ for fixed charge multiplicity increases for increasing energy, while the decrease of $\langle p_T \rangle$ with increasing multiplicity becomes weaker as the energy increases.

(g) The shape of the charge distribution for pion fragmentation appears to remain the same as the incident-beam momentum increases from 16 to 100 GeV/c.

(h) The charge fragmentation distribution from the target proton is narrower than that from the fragmentation of a projectile pion.

ACKNOWLEDGMENT

We are pleased to acknowledge the assistance of the staff of the Fermi National Accelerator Laboratory, the 30-inch bubble-chamber staff and the Neutrino Lab personnel in particular, in obtaining these exposures. We thank the Proportional Hybrid Consortium for the use of the upstream proportional wire chambers as part of the beam-particle identification tagging system. We also acknowledge the efforts of our scanning and measuring staff.

---

*Work supported in part by the National Science Foundation.

†Present address: Brookhaven National Laboratory, Upton, N. Y. 11973.

‡Work supported in part by the U. S. Energy Research and Development Administration.

§Present address: Pfizer Medical Systems, Columbia, Md., 21045.

[1]P. Bosetti, H. Grassler, H. Kirk, M. Matziolis, U. Gensch, P. Kostka, K. Bockmann, G. J. Bossen, J. Lowsky, M. Rost, T. Besliu, V. T. Cocconi, P. F. Dalpiaz, P. Duinker, S. Matsumoto, D. R. O. Morrison, R. Stroynowski, H. Wahl, T. Coghen, W. Zielinski, S. Brandt, M. Bardadin-Otwinowska, and T. Hofmokl, Nucl. Phys. B54, 141 (1973).

[2]J. T. Powers, N. N. Biswas, N. M. Cason, V. P. Kenney, and W. D. Shephard, Phys. Rev. D 8, 1947 (1973); P. T. Go, W. D. Shephard, V. P. Kenney, J. M. Bishop, N. N. Biswas, and N. M. Cason, *ibid.* 11, 3092 (1975).

[3]D. J. Crennell, H. A. Gordon, M. L. Ioffredo, and K-W. Lai, Phys. Rev. Lett. 28, 643 (1972).

[4]W. Morris, B. Y. Oh, D. L. Parker, G. A. Smith, J. Whitmore, L. Voyvodic, R. Walker, R. Yaari, E. W. Anderson, H. B. Crawley, W. J. Kernan, F. Ogino, R. G. Glasser, D. G. Hill, G. McClellan, H. L. Price, B. Sechi-Zorn, G. A. Snow, F. Svrcek, W. D. Shephard, J. M. Bishop, N. N. Biswas, N. M. Cason, E. D. Fokitis, and V. P. Kenney, Phys. Lett. 56B, 395 (1975).

[5]E. L. Berger, V. T. Cocconi, M. J. Counihan, T. Coghen, U. Gensch, V. Karimaki, G. Kellner, A. Kotanski, D. Kuhn, D. R. O. Morrison, P. Schmidt, D. Sotiriou, R. Stroynowski, F. A. Triantis, and H. Wahl, Nucl. Phys. B77, 365 (1974).

[6]J. Erwin, J. H. Klems, W. Ko, R. L. Lander, D. E. Pellett, P. M. Yager, and M. Alston-Garnjost, Phys. Rev. Lett. 32, 254 (1974).

[7]We thank these groups, Dr. Morrison and Dr. Lander in particular, for their cooperation in giving the film to our groups.

[8]W. M. Morse, V. E. Barnes, D. D. Carmony, R. S. Christian, A. F. Garfinkel, L. K. Rangan, A. R. Erwin, E. H. Harvey, R. J. Loveless, and M. A. Thompson, Phys. Rev. D 15, 66 (1977).

[9]V. E. Barnes, D. D. Carmony, R. S. Christian, A. F. Garfinkel, W. M. Morse, T. A. Mulera, L. K. Rangan, R. N. Diamond, A. R. Erwin, E. H. Harvey, R. J. Loveless, M. A. Thompson, and D. R. Winn, Phys. Rev. Lett. 34, 415 (1975).

[10]G. A. Smith, in *Particles and Fields*—1973, proceedings of the Berkeley Meeting of the Division of Particles and Fields of the APS, edited by H. H. Bingham, M. Davier and G. Lynch (AIP, New York, 1973), p. 500.

[11]J. Benecke, T. T. Chou, C. N. Yang, and E. Yen, Phys. Rev. 188, 2159 (1969).

[12]R. Schindler, C. Bromberg, D. Chaney, T. Ferbel, P. Slattery, J. Cooper, and A. Seidl, Phys. Rev. Lett. 33, 862 (1974).

[13]J. T. Powers *et al.*, Ref. 2; P. T. Go *et al.*, Ref. 2; V. P. Kenney (private communication); E. O. Abdrakhmanov *et al.*, Ref. 18; D. J. Crennell *et al.*, Ref. 3; S. L. Stone, D. Cohen, T. Ferbel, P. F. Slattery, B. Werner, W. Barletta, M. Johnson, T. Ludlam, A. J. Slaughter, and H. D. Taft, Phys. Rev. D 7, 3532 (1973); M. E. Law, J. Kasman, R. S. Panvini, W. H. Sims and T. Ludlam, Report No. LBL-80, 1972 (unpublished); M. Alston-Garnjost, K. W. Barnham,

M. S. Rabin, A. Barbaro-Galtieri, S. M. Flatte, J. H. Friedman, G. R. Lynch, J. N. MacNaughton, F. T. Solmitz, C. Risk, W. D. Shephard, J. T. Powers, N. N. Biswas, N. M. Cason, V. P. Kenney, and D. W. Thomas, Phys. Lett. 39B, 402 (1972).

[14]C. Quigg (private communication); C. Quigg and E. Rabinovici, Phys. Rev. D 13, 2525 (1976).

[15]Chan Hong-Mo, C. S. Hsue, C. Quigg, and J. M. Wang, Phys. Rev. Lett. 26, 672 (1971).

[16]H.I. Miettinen, Phys. Lett. 38B, 431 (1972).

[17]J. Whitmore, W. Morris, B. Y. Oh, D. L. Parker, and G. A. Smith, Phys. Lett. 60B, 211 (1976); E. W. Beier *et al.*, Phys. Rev. Lett. 37, 1120 (1976).

[18]E. O. Abdrakhmanov *et al.*, Nucl. Phys. B72, 189 (1974).

[19]V. P. Kenney *et al.*, (Notre Dame, Duke, Institute of Particle Physics of Canada Collaboration) paper submitted to the Seattle APS DPF Meeting, 1975 (unpublished).

[20]J. Whitmore, Phys. Rep. 27C, 187 (1976).

[21]T. Ferbel, Phys. Rev. Lett. 29, 448 (1972); Phys. Rev. D 8, 2321 (1973).

[22]P. Lauscher *et al.*, Nucl. Phys. B106, 31 (1976); presented in U. Idschok *et al.*, Nucl. Phys. B67, 93 (1973).

[23]P. Bosetti *et al.*, Nucl. Phys. B62, 46 (1973).